Delay Performance of Different MAC Schemes for Multihop Wireless Networks

Min Xie and Martin Haenggi
Department of Electrical Engineering
University of Notre Dame
Notre Dame, IN 46556, USA
Email: {mxie,mhaenggi}@nd.edu

***Abstract*— This paper studies the end-to-end (e2e) delay performance of a multihop wireless network fed with a single constant bit rate (CBR) source. Two MAC schemes are investigated, m-phase TDMA and probabilistic slotted ALOHA. A delay model is used to analyze the resulting tandem queueing system and derive tight upper bounds on the delay mean. The e2e delay linearly increases with the route length and its distribution converges to a Gaussian distribution. For channels with reception probability greater than 0.5, TDMA significantly outperforms ALOHA. For unreliable channels, the situation is less clear.**

I. Introduction

Nowadays many wireless applications demand delay guaranteed services, which is more challenging than in the wired network because of the random delay incurred by the error-prone wireless channel. In order to provide such QoS guarantees, it is important to know the system performance. The subject of this paper is the analysis of the delay performance of multihop wireless networks fed with a single CBR source.

Regarding the e2e delay, we take into account both the transmission delay and queueing delay [1]. The multihop topology makes the e2e delay jointly affected by several factors, including the *routing algorithm*, the *scheduling policy*, and the *MAC scheme*. We concentrate on the impact of MAC schemes. The assumption of a single CBR flow makes a simple FIFO discipline sufficient for packet scheduling. Moreover, the multihop network contains only one active route such that the topology is essentially reduced to one dimension (1-D). The resulting performance provides an upper bound for 2-D networks with multiple active routes. Two MAC schemes are considered, i) deterministic m-phase TDMA, in which a node is allocated to transmit once in m time slots and nodes m hops apart can transmit simultaneously; and ii) probabilistic slotted ALOHA, in which every node independently decides to transmit with probability $1/m$ if it has packets buffered.

From a queueing perspective, the 1-D network, referred to as line network, is a tandem system. So, this paper focuses on the *wireless MAC scheme* and the *tandem queueing system*.

Many analyses of MAC schemes are based on a single-hop topology and the "infinite population model" [2]–[6]. The infinite population model assigns a new node to a new arriving packet, and the transmission attempts in the network are Poisson distributed with the spatial density of nodes. This model excludes the queueing delay and accounts only for the transmission delay and access delay. In contrast, the analysis of tandem queueing systems focuses on the queueing delay [7]–[10]. The channel is generally set to be error-free so that the access and transmission delay incurred by MAC-dependent collision and interference can be ignored.

Our main contribution is to *jointly* analyze the tandem system and the MAC scheme in the wireless environment. Both the queueing delay and transmission/access delay are taken into account. An upper bound on the e2e delay is derived. With a single CBR source, the delays experienced at a single node converge to a geometric distribution, and the e2e delay converges to a Gaussian distribution. The delay means and variances are linear in the route length, and we also conclude that the delay is very sensitive to the channel reception probability.

II. Analysis of the m-phase TDMA system

The line network is a chain of $N+1$ single-server nodes using the FIFO service discipline. Node 1 is the source node that generates fixed-length packets at a constant rate $1/r$, $r \in \mathbb{N}$, *i.e.*, one packet in r time slots. Node $N+1$ is the destination. All remaining nodes are pure relays. The channel is slotted to one packet duration. Transmission attempts are made at the slot boundaries. As in [5], [6], the channel error is characterized by the reception probability p_r, which depends on the received signal-to-noise-and-interference ratio (SNIR) and the predetermined SNIR threshold for a successful reception. Failed packets will be retransmitted until successfully received.

The m-phase TDMA scheduler lets nodes $i, m+i, 2m+i, \ldots$ $(1 \le i \le m)$ transmit simultaneously at times $i, m+i, 2m+i, \ldots$ and so on. A transmission can be either a transmission of new packet or retransmission of a failed packet. The time is divided into frames of m time slots, where $m < r$ for stability. Considering a heavy traffic load, we assume $m < r < 2m$. For a node, the beginning of a frame is the beginning of the time slot allocated to this node. If we

observe the system at the frame level, the transmission time is geometric with p_r. For simplicity, we denote the geometric distribution with parameter p_r by $\mathcal{G}_{p_r}$. The traffic intensity is defined by $\rho = m/(p_r r) < 1$.

We start the analysis with the source node.

A. Delay distribution of the first node

At the frame level, the service time is $\mathcal{G}_{p_r}$. For $m < r < 2m$, the interarrival time r/m is not an integer in terms of frame. The number of arrivals in one frame jumps between 0 and 1 and depends on the arrivals of all previous $r-1$ frames, which makes it difficult to use the conventional approach of establishing a Markov chain to keep track of the buffer size. To take advantage of the constant interarrival time, we resort to a delay model that was first used in [11]. The system state is denoted by the current delay of the Head-of-Line (HOL) packet in terms of time slots although the state transitions occur at the frame boundaries. The transition probability from state i to state j is:

$$P_{ij} = \begin{cases} p_r & i \geq 0, \quad j = i - \Delta, \quad \Delta := r - m \\ 1 - p_r & i \geq 0, \quad j = i + m, \\ 1 & i < 0, \quad j = i + m. \end{cases} \tag{1}$$

The absolute value of the negative state indicates the remaining time prior to the arrival of the next packet. Surely, the server is idle when the system state is negative. Given $r < 2m$, the server idle time does not exceed one frame.

At frame t, let the HOL packet be packet k and its delay be $d_k(t)$. Packet k is transmitted at the beginning of frame t. If the transmission is successful, packet k departs and packet $k+1$ becomes the HOL packet at frame $t+1$. The delay of packet $k+1$ at frame t is $d_{k+1}(t) = d_k(t) - r$. It increases by m up to $d_{k+1}(t+1) = d_k(t) - r + m = d_k(t) - \Delta$ at frame $t+1$. That is, the system state transits from $i = d_k(t)$ to $j = d_k(t) - \Delta$ with probability p_r. If $j < 0$, packet k is the last queued packet and the buffer becomes empty after packet k's departure. Since the server idle time is bounded by one frame, a new packet will arrive in the middle of frame $t+1$. This new packet will wait $m - |j| > 0$ slots before it is able to access the channel at the next frame. Then the negative state j transits to a positive state $m - |j|$ with probability 1. If the transmission is failed (with probability $1 - p_r$), the HOL packet remains at the buffer and is retransmitted at frame $t+1$, with its delay increased by m to $d_k(t+1) = d_k(t) + m$.

Denote the steady-state probabilities by $\{\pi_i | i \geq -\Delta\}$. From (1), we derive the generating function (z-transform) $G(z)$

$$G(z) = \frac{\sum_{h=-\Delta}^{-1} \pi_h z^h}{1 - \frac{z^\Delta}{p} \frac{1 - z^m}{1 - z^{m+\Delta}}}. \tag{2}$$

Based on $G(1) = 1$, we can calculate the average server idle time $P_I = \sum_{i=-\Delta}^{-1} \pi_i$ as follows:

$$P_I = G(z)|_{z=1} \lim_{z \to 1} \left(1 - \frac{z^\Delta}{p} \frac{1 - z^m}{1 - z^{m+\Delta}}\right) = 1 - \rho. \tag{3}$$

The average server busy time is $P_B = \rho$. Besides, the average departure rate $P_B p_r = m/r$ is consistent with the expected arrival rate in terms of frames.

If the transmission is successful, the HOL packet departs the node with a delay as the sum of the system state and one slot for transmission. The delay distribution $\{d_i^{(1)} | i \geq 1\}$ is

$$d_i^{(1)} = \frac{\pi_{i-1} p_r}{\sum_{j=0}^{\infty} \pi_j p_r} = \frac{\pi_{i-1}}{\sum_{j=0}^{\infty} \pi_j}. \tag{4}$$

Specifically, for $\Delta = 1$, (1) leads to

$$\pi_i = \begin{cases} p_r \pi_{i+1} & 0 \leq i < m-1 \\ p_r \pi_{i+1} + p_r \pi_0 & i = m-1 \\ p_r \pi_{i+1} + (1 - p_r) \pi_{i-m} & i \geq m. \end{cases} \tag{5}$$

These equations also hold if π_i is replaced by $d_{i+1}^{(1)}$. Then the delay distribution can be recursively derived with respect to $d_1^{(1)}$. The generating function of $\{d_i^{(1)}\}$ is

$$G_D(z) = \frac{(z^m - 1)}{z - p_r - (1-p) z^{m+1}} \cdot \frac{1 - \rho}{\rho}, \tag{6}$$

resulting in a delay mean

$$\overline{D}_1 = \frac{1}{2(1-\rho)}. \tag{7}$$

Fig. 1 compares the simulation result with the analytical delay distribution given by (1) and (4) for a system with $m = 3, r = 4, p_r = 0.8$. Our queueing analysis accurately characterizes the delay performance of the source node.

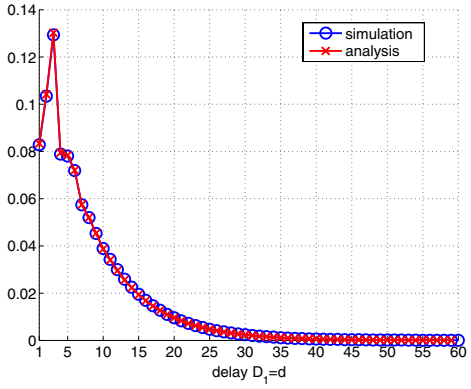

Fig. 1. Delay probabilities of the source node in the TDMA system

B. Delay distribution of the relay nodes

The output of node 1 is the input to node 2. We characterize this output process by the interdeparture time $T^{(1)}$. Due to the frame structure, the packet departs only at the frame boundary, which allows us to observe and measure the interdeparture time at the frame level.

The packet transmission time is $S^{(1)} \sim \mathcal{G}_{p_r}$ in terms of frames. Observing at the packet departing instant, if the queue is non-empty (probability $\widetilde{P}_B$), the interdeparture time is $S^{(1)}$; otherwise, the interdeparture time is $S^{(1)}$ plus the server idle

time of one frame. Note that P_B and $\widetilde{P}_B$ are the server busy probability observed at any frame and at the packet departing frame, respectively. Since the arrival process is not memoryless, $\widetilde{P}_B \neq P_B$. Using the generating function of $T^{(1)}$, we derive the interdeparture time distribution $\{t_i^{(1)}\}$:

$$t_i^{(1)} = \begin{cases} \widetilde{P}_B p_r & i = 1 \\ p_r(1-p_r)^{i-2}(1-\widetilde{P}_B p_r) & i > 1 \end{cases} \quad (8)$$

Since the average interdeparture time is equal to the interarrival time r/m, we have

$$\widetilde{P}_B p_r = 1 + p_r - \frac{1}{\rho} = 1 - \frac{p_r}{m}. \quad (9)$$

The distribution (8) corresponds to a correlated on-off process, which is characterized by a transition matrix (see [11, Eqn.(1)]). In our case, the transition probabilities are $a_{01} = p_r$ and $a_{10} = p_r/m$. Correlation and burstiness are induced in the output process even though the channel errors are independent and the input process is smooth.

Node 2 (the first relay node) is characterized as a queueing system with a correlated on-off source and a geometric server. A similar system is analyzed in [11], in which the maximum delay is bounded. We extend the result to the case of infinite delay and conclude that the delay of node 2 is geometrically distributed in terms of frames. In terms of time slots, the delay distribution is

$$d_i^{(2)} = \begin{cases} (1-x)x^j & \text{if} \quad i = jm+1, j \geq 0 \\ 0 & \text{otherwise} \end{cases} \quad (10)$$

where

$$x = \frac{m(1-p_r)}{m(1-p_r)^2 + p_r^2} < 1,$$

and the delay mean is

$$\overline{D}_2 = 1 + m\frac{\rho}{1-\rho}\frac{1-p_r}{p_r}. \quad (11)$$

C. End-to-end delay

Simulation results (Fig. 3(a)) confirm that the relay-node delay converges to a geometric distribution and the e2e delay converges to a Gaussian distribution. This observation allows us to approximate the delay of the individual relay nodes by the geometric distribution given in (10).

The end-to-end delay is the sum of the individual node delays, *i.e.*, $D = \sum_{i=1}^{N} D_i$. Approximately, D_i $(i > 2)$ can be upper bounded by D_2, the local delay at the first relay node. Therefore, the delay mean is uppoer bounded by

$$\begin{aligned} \overline{D} &\leq \overline{D}_1 + (N-1)\overline{D}_2 \\ &= \frac{1}{2(1-\rho)} + (N-1)(1 + m\frac{\rho}{1-\rho}\frac{1-p_r}{p_r}). \end{aligned} \quad (12)$$

Fig. 4(a) is a comparison of this upper bound (12) with the simulation result.

III. Analysis of the probabilistic slotted ALOHA MAC scheme

m-phase TDMA incurs a substantial amount of overhead to establish the frame structure. Therefore, we consider the probabilistic slotted ALOHA, in which every node independently and probabilistically determines whether to transmit. To compare with the TDMA scheme, we set the transmit probability to be $1/m$. The traffic and channel model remain unchanged. Again, we start with the source node.

A. Delay distribution of the first node

Unlike the TDMA system, the ALOHA system is observed at the slot level. With the channel reception probability p_r, a packet is correctly received if and only if the node attempts to transmit and the transmission is successful, with probability $s = p_r/m$ (given the assumption that the arrival and transmission are independent). Otherwise, the transmission fails. The transmission time is $\mathcal{G}_s$. We employ the delay model again and denote the system state by the current delay of the HOL packet. The state transition probabilities are

$$P_{ij} = \begin{cases} 1-s & i \geq 0, \quad j = i+1 \\ s & i \geq 0, \quad j = i-(r-1) \\ 1 & i < 0, \quad j = i+1. \end{cases} \quad (13)$$

Since the maximum interval between a packet departure and the next packet arrival is $(r-1)$ slots, the minimum negative state is $-(r-1)$. Rewriting the balance equations, we obtain

$$\pi_i = s\sum_{j=k}^{r-1+i} \pi_j, \quad i \geq -(r-1), \quad k = \max\{0, i\}, \quad (14)$$

From (14), we deduce the system busy probability $P_B = \sum_{i=0}^{\infty}\pi_i = 1/(sr) = \rho$, which is identical to the busy probability of the TDMA system. A possible solution to (14) is the geometric distribution $\pi_i = \alpha^i\pi_0$ for all $i \geq 0$. Since $\sum_i \pi_i = 1$ and $P_B = 1/sr$, α is a positive real root of the polynomial

$$y^r - \frac{y}{s} + \frac{1}{s} - 1 = 0. \quad (15)$$

Based on Descartes' Sign Rule and $1/s > 1$, there are exactly two positive real roots irrespective of r. The desired root α lies between 0 and 1. The delay distribution $\{d_i^{(1)}\}$ is expressed in terms of $\{\pi_i | i \geq 0\}$ using (4), which leads to $d_i^{(1)} = (1-\alpha)\alpha^{i-1}$ $(i \geq 1)$. Fig. 2 shows the simulated delay distribution for a system with $m = 3, r = 4, p_r = 0.8$, in which the parameter $\alpha = 0.9569$ is very close to the solution $\alpha = 0.9571$ of (15). We also derive that the delay mean $\overline{D}_1 = 1/(1-\alpha)$ can be approximated as

$$\overline{D}_1 \approx \frac{m\rho}{2(1-\rho)}. \quad (16)$$

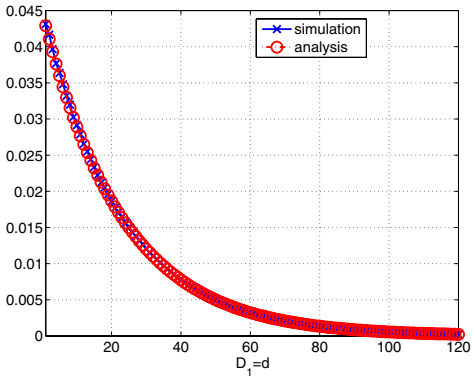

Fig. 2. Delay probabilities of the source node in the ALOHA system

B. Delay distribution of the relay nodes

The analysis of the output process of the source node is more complicated for ALOHA since the server idle time ranges between 0 and $(r-1)$ slots. We establish a new queueing model to characterize the interdeparture time.

Instead of observing the system at every time slot, we observe the moment when the HOL packet departs. The system state is denoted by the delay of the next HOL packet. The state transition probabilities are:

$$P_{ij}^{out} = s(1-s)^{r-k+j-1}, \quad k = \max\{0, i\}. \tag{17}$$

The balance equations for all $i \geq -(r-1)$ are

$$\pi_i^{out} = s \sum_{j=i}^{i+r-1} \pi_j^{out}. \tag{18}$$

Similar to (14), a solution to (18) is the geometric distribution $\pi_i^{out} = (1-\beta)\beta^{r+i-1}$. After some manipulations, it can be established that $\beta = \alpha$. Then, the interdeparture time $T^{(1)}$ is

$$T^{(1)} = \begin{cases} i+S & \text{with probability } \pi_{-i}^{out} \\ S & \text{with probability } P_B^{out}, \end{cases} \tag{19}$$

where $S \sim \mathcal{G}_s$, and $P_B^{out} = \sum_{i\geq 0} \pi_i^{out} = \alpha^{r-1}$ is the server busy rate. The distribution $\{t_i^{(1)}\}$ is

$$t_i^{(1)} = \frac{s\Big(s\alpha^r(1-s)^{i-1} + (1-\alpha)\alpha^{r-k}(1-s)^{i-k}\Big)}{1-\alpha(1-s)}, \tag{20}$$

where $k = \min\{r, i\}$. In order to compare with the TDMA system, we approximate (20) by a correlated on-off process. Given $t_1^{(1)} = (s+\alpha-1)/\alpha$ and the condition that the mean $\overline{T}_1 = r$, we obtain a transition matrix, where $a_{10} = (1-s)/\alpha$ and $a_{01} = (1-s)/((r-1)\alpha)$. Then, the delay distribution of node 2 is approximated by a geometric distribution with $x = (1-s)/(sa_{10} + (1-s)a_{00})$. The delay mean is

$$\overline{D}_2 = 1 + m\frac{\rho}{1-\rho}\alpha. \tag{21}$$

C. End-to-end delay

As shown in Fig. 3(b), the e2e delay converges to a Gaussian distribution. We approximate the delay of a relay node by the geometric distribution of node 2. Again, the e2e delay is upper bounded by the sum of all node delays. With an approximation of (16), the delay mean is upper bounded by

$$\begin{aligned} \overline{D} &\leq \frac{1}{1-\alpha} + (N-1)(1 + m\frac{\rho}{1-\rho}\alpha) \\ &\approx \frac{m}{2}\frac{\rho}{1-\rho} + (N-1)(m\frac{\rho}{1-\rho} - 1). \end{aligned} \tag{22}$$

If N is large, $\overline{D}$ is mainly affected by the delay mean of the relay nodes. Recalling (11) and (21), we are able to compare the delay mean between two MAC schemes,

$$\frac{\overline{D}^{\text{TDMA}}}{\overline{D}^{\text{ALOHA}}} \approx \frac{1-p_r}{p_r}\frac{1}{\alpha} \approx \frac{1-p_r}{p_r}, \tag{23}$$

where the second approximation holds when the traffic load is high and thus $\alpha \approx 1$.

IV. Simulation Results

This section presents a set of simulation results to confirm the analyses in Section II and III. We first consider the e2e delay distribution (from the source node to different relay nodes) of a line network with $m = 3, r = 4, p_r = 0.8, N = 8$ (shown in Fig. 3). For both MAC schemes, the delay distribution converges to a Gaussian distribution.

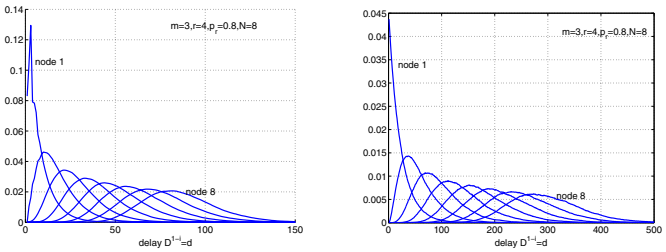

(a) TDMA (b) ALOHA

Fig. 3. Probability distributions of the e2e delay

Fig. 4 compares the analytical upper bounds (12) and (22) with the simulation result, showing that the bounds are comparatively tight. The e2e delay mean increases linearly with the number of nodes. The deviation from strict linearity is caused by the non-geometric output process of the first node. Further, the delay mean ($\overline{D} = 292$) of the ALOHA system is about 4 times that of the TDMA system ($\overline{D} = 85$) in agreement with our analysis (23): $p_r/(1-p_r) = 4$ for $p_r = 0.8$. In the ALOHA network, the drastic increase in the delay is caused by the lack of central control and the resulting reduction of spatial reuse.

To discuss the impact of p_r, Figs. 5 and 6 exhibit the delay mean and variance for different p_r in a network with $m =$

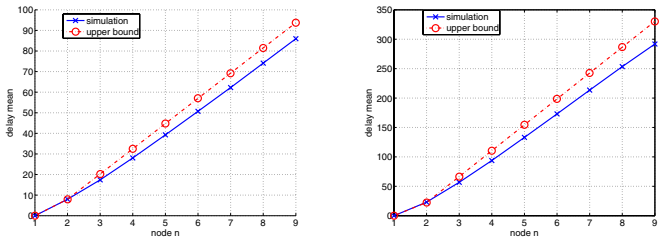

(a) TDMA (b) ALOHA

Fig. 4. Comparison of the e2e delay mean

$4, r = 7, N = 12$. When p_r is closer to the traffic load 0.6, both the mean and variance increase substantially.

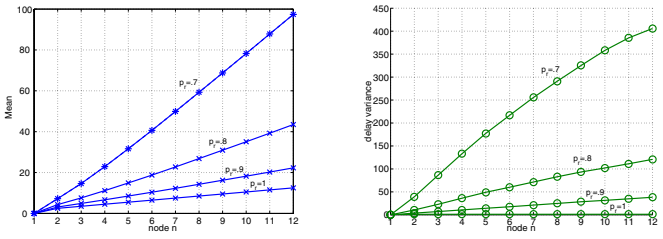

(a) Delay mean (b) Delay variance

Fig. 5. Comparison of delay performance of TDMA

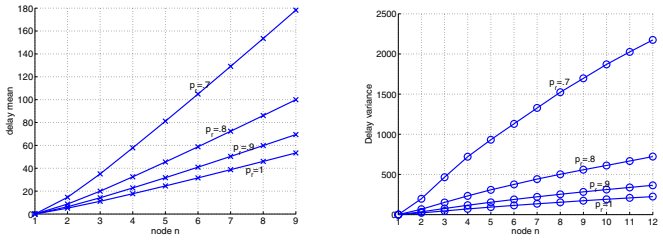

(a) Delay mean (b) Delay variance

Fig. 6. Comparison of delay performance of ALOHA

V. Conclusion

For both MAC schemes, the delay performance is sensitive to the reception probability p_r, particularly when p_r is close to the normalized traffic load. Besides, the e2e delay mean and variance linearly increase with the number of nodes. Such linearity allows us to regard these nodes as almost independent and analyze them individually. The relay-node delay distribution converges to a geometric distribution. Thus, if the path is long, the e2e delay distribution is well approximated by a Gaussian distribution.

We derived an upper bound on the e2e delay mean for both MAC schemes. When the traffic load is heavy, the delay mean of the ALOHA network is approximately $p_r/(1-p_r)$ times than that of the TDMA network. Therefore, for a channel sufficiently good, say $p_r > 0.5$, TDMA outperforms ALOHA in both throughput and delay. However, if the channel is not as good as expected, saying $p_r < 0.5$, ALOHA is more efficient to take advantage of the random channel errors and achieves a smaller delay than TDMA. Note that in practice, due to interference, p_r of the TDMA system is higher than that of the ALOHA system if both systems are optimized [12], which enhances the benefits of using TDMA. Our future work is to analyze the delay performance of MAC schemes in association with the fading channel characteristics.

Acknowledgment

The authors would like to thank the support of the Center for Applied Mathematics (CAM) Fellowship of the University of Notre Dame and the partial support of NSF (grant ECS03-29766).

References

[1] C.-K. Toh, Minar Delwar, and Donald Allen, "Evaluating the Communication Performance of an Ad Hoc Wireless Network," *IEEE Transactions on Wireless Communications*, vol. 1, no. 3, pp. 402–414, July 2002.

[2] Jens C. Arnbak and Wim Van Blitterswijk, "Capacity of Slotted ALOHA in Rayleigh-Fading Channels," *IEEE Journal on Selected Areas in Communications*, vol. 5, no. 2, pp. 261–269, Feb. 1987.

[3] Malcolm C. H. Peh, Stephen V. Hanly, and Philip Whiting, "Random Access with Multipacket Reception over Fading Channels," in *Australian Communications Theory Workshop 2003*, Feb. 2003.

[4] Flaminio Borgonovo and Michele Zorzi, "Slotted ALOHA and CDPA: A Comparison of Channel Access Performance in Cellular Systems," *ACM Wireless Networks*, vol. 3, no. 1, pp. 43–51, Mar. 1997.

[5] Yang Yang and Tak-Shing Peter Yum, "Delay Distributions of Slotted ALOHA and CSMA," *IEEE Transactions on Communications*, vol. 51, no. 11, pp. 1846–1857, Nov. 2003.

[6] Michele Zorzi and Silvano Pupolin, "Slotted ALOHA for High-Capacity Voice Cellular Communications," *IEEE Transactions on Vehicular Technology*, vol. 43, no. 4, pp. 1011–1021, Nov. 1994.

[7] John A. Morrison, "Two Discrete-Time Queues in Tandem," *IEEE Transactions on Communications*, vol. 27, no. 3, pp. 563–573, Mar. 1979.

[8] J. Hsu and P. J. Burke, "Behavior of Tandem Buffers with Geometric Input and Markovian Output," *IEEE Transactions on Communications*, vol. 24, no. 3, pp. 358 – 361, Mar. 1976.

[9] Moshe Sidi, "Tandem Packet-Radio Queueing Systems," *IEEE Transactions on Communications*, vol. 35, no. 2, pp. 246–248, Feb. 1987.

[10] Michael J. Neely, "Exact Queueing Analysis of Discrete Time Tandems with Arbitrary Arrival Processes," in *ICC*, 2003, vol. 4, pp. 2221 – 2225.

[11] Kelvin K. Lee and Samuel T. Chanson, "Packet Loss Probability for Bursty Wireless Real-Time Traffic Through Delay Model," *IEEE Transactions on Vehicular Technology*, vol. 53, no. 3, pp. 929–938, May 2004, correspondence.

[12] Martin Haenggi, "On the Local Throughput of Large Interference-Limited Wireless Networks," in *39th Annual Conference on Information Sciences and Systems (CISS'05)*, Baltimore, MD, Mar. 2005.